Interaction between Hurricane Florence (1988) and an Upper-Tropospheric Westerly Trough

JAINN JONG SHI

Science Applications International Corporation, McLean, Virginia

SIMON CHANG

Naval Research Laboratory, Monterey, California

SETHU RAMAN

Department of Marine, Earth and Atmospheric Sciences, North Carolina State University, Raleigh, North Carolina

(Manuscript received 7 August 1995, in final form 18 October 1996)

ABSTRACT

The Naval Research Laboratory's limited-area numerical prediction system, a version of Navy Operational Regional Atmospheric Prediction System, was used to investigate the interaction between Hurricane Florence (1988) and its upper-tropospheric environment. The model was initialized with the National Meteorological Center (now the National Centers for Environmental Prediction)/Regional Analysis and Forecasting Systems 2.5° analysis at 0000 UTC 9 September 1988, enhanced by a set of Omega dropwindsonde data through a three-pass nested-grid objective analysis.

Diagnosis of the 200-mb level structure of the 12-h forecast valid for 1200 UTC 9 September 1988 showed that the outflow layer was highly asymmetric with an outflow jet originating at approximately 3° north of the storm. In agreement with the result of an idealized simulation (Shi et al. 1990), there was a thermally direct, circum-jet secondary circulation in the jet entrance region and a thermally indirect one in a reversed direction in the jet exit region. In several previous studies, it was postulated that an approaching westerly jet had modulated the convection and intensity variations of Florence. In a variational numerical experiment in this study, the approaching westerly jet was flattened out by repeatedly setting the jet-level meridional wind component and zonal temperature perturbations to zero in the normal mode initialization procedure. Compared with the control experiment, the variational experiment showed that the sudden burst of Florence's inner core convection was highly correlated with the approaching upper-tropospheric westerly jet. These experiments also suggested that the approaching upper-tropospheric westerly jet was crucial to the intensification of Florence's inner core convection between 1000 and 1500 UTC 9 September, which occurred prior to the deepening of the minimum sea level pressure (from 997 to 987 mb) between 1200 UTC 9 September and 0000 UTC 10 September.

Many earlier studies have attempted an explanation for the effect on tropical cyclones of upper-tropospheric forcings from the eddy angular momentum approach. The result of this study provides an alternative but complementary mechanism of the interaction between an upper-level westerly trough and a tropical cyclone.

1. Introduction

Numerous observational and numerical modeling studies during the past 40 years have tremendously increased our understanding of tropical cyclones. The adoption of satellite data also helps forecasters and researchers to track the movement and intensity of tropical cyclones. Still, compared to the understanding of mid-latitude weather systems, most of the structure and behavior of tropical cyclones are still not fully understood, mainly because of the insufficient observational data over the vast tropical ocean. Past studies (Black and Anthes 1971; Sadler 1976, 1978; Frank 1977b; Tuleya and Kurihara 1981; Pfeffer and Challa 1981; Merrill 1984; Holland and Merrill 1984; Chen and Gray 1984; Ooyama 1987; Merrill, 1988a,b; Molinari and Vollaro 1989, 1990; Kaplan and Franklin, 1991; Shi et al. 1990; Rodgers et al. 1991; DeMaria et al. 1993) have demonstrated that the movement and growth of tropical cyclones are affected by the interaction between the outflow layer of tropical cyclones and its environmental flows. For example, Holland and Merrill (1984) pointed out that the strong cyclonic vorticity in the lower and middle troposphere in an intense tropical cyclone becomes more stable and likely more resistant to envi-

Corresponding author address: Dr. Jainn Jong Shi, Naval Research Laboratory, 4555 Overlook Ave., SW, Code 7225,Washington, DC 20375-5000.
E-mail: shi@metcomp.nrl.navy.mil

ronmental forcing, whereas the upper-tropospheric anticyclonic, asymmetric outflow is not as stable inertially (Black and Anthes 1971), and therefore is less resistant to the environmental forcing. Thus, the movement and intensity of an intense tropical cyclone would probably respond more rapidly to upper-tropospheric forcings. An improved understanding of the structure of the outflow layer of tropical cyclones may be important in predicting tropical cyclone intensification and motion.

Real data analysis of the outflow layer of the tropical cyclone is almost impossible because of the sparsity of the observational data over the tropical ocean. Even when some observational data are available, the studies still suffer from not having frequent enough data to construct a chain of events or to establish a cause–effect relationship. Much of our knowledge has come from composite studies (Black and Anthes 1971; Sadler 1976, 1978; McBride 1981; Chen and Gray 1984; Merrill 1988a,b; DeMaria et al. 1993), a few case studies (Molinari and Vollaro 1989, 1990; Kaplan and Franklin 1991; Rodgers et al. 1991), or some idealized model studies (Tuleya and Kurihara 1981; Pfeffer and Challa 1981; Ooyama 1987; Shi et. al 1990). Based on these studies, our knowledge of the structure of the outflow layer of tropical cyclones and the plausible mechanism through which the interaction with the upper troposphere occurs are summarized as follows.

a. Structure of the outflow layer of tropical cyclones

The outflow layer of the tropical cyclone is comparatively shallow, generally confined between 100 and 300 mb (Frank 1977a). The asymmetric outflow of the tropical cyclone is characterized by outflow jets. Chen and Gray (1984) asserted that the outflow jets help to remove mass from the central region and transport the warm and dry air to outer regions, maintaining the convective instability in the inner core region. Merrill (1984) observed that the outflow from a hurricane concentrates into one or two outflow maxima or channels. The wind maximum in the outflow layer can normally be found to the north or northwest of the storm center in the Northern Hemisphere. He noted that the appearance of outflow channels is similar to that of the "jet streaks," that are commonly observed in association with the midlatitude troughs. He also speculated that the upper-tropospheric, baroclinic processes may be important in the hurricane outflow jet streak, and there may be a possible secondary circulation around the outflow layer, similar to the jet streak in midlatitudes. Ooyama (1987) was able to generate the asymmetric outflow in various environmental flows in a simple two dimensional (in the x and y directions) model of the outflow layer using shallow water equations with a prescribed updraft carrying mass and momentum. Previous numerical study by Shi et al. (1990) demonstrated the existence of a circum-jet secondary circulation at the entrance region of the outflow jet. The circum-jet secondary circulation at the entrance region is thermally direct with the ascending branch located on the anticyclonic shear side, and the descending branch located at the cyclonic shear side of the outflow jet. Molinari and Vollaro (1989) also speculated that the upward motion constantly occurs at radii inside the outflow maximum. In a composite study, Merrill (1988a) found that the upper-tropospheric circulation associated with a hurricane is clearly visible on the synoptic scale with a substantial asymmetric component of both radial and tangential winds. However, he also stated that the outward branch of the hurricane's secondary circulation, found in the outflow layer between 100 and 300 mb, may not be all originated from the hurricane.

b. Angular momentum transport in the outflow layer

Pfeffer (1958) proposed that eddy angular momentum is transferred into the core of the hurricane with a net positive (cyclonic) contribution to the angular momentum budget. Black and Anthes (1971) found an anticyclonic eddy to the right and a cyclonic eddy to the left of the storm motion, which transport a significant amount of negative (positive) relative angular momentum outward (inward). Anthes (1974) further demonstrated that the outflow layer of actual storms exhibits a great degree of asymmetry as indicated by a sizable horizontal eddy angular momentum flux. He also noted that a large import of angular momentum is required to offset frictional loss to the sea. To further augment this point, intense and well-organized inward eddy angular momentum flux was found in developing Atlantic hurricanes, and weak and poorly organized flux was found in nondeveloping disturbances by Pfeffer and Challa (1981). In their model study, they showed that a weak disturbance is not capable of developing into a hurricane solely by the Ekman pumping and cooperative instability without the help of the observed convergence of eddy momentum flux.

Holland (1983), in his composite study, found that the azimuthal eddy transport of angular momentum is effective at large radii in the outflow layer for a developed cyclone, while the mean transverse circulation dominates the inner region. Using a 5-year composite of Atlantic hurricanes, Merrill (1988a) found sizable eddy import of angular momentum in the outflow layer. However, he also quickly pointed out that there is no clear relationship between eddy angular momentum flux and intensity changes of hurricanes. He speculated that any benefits to the hurricane from the eddy angular momentum flux will be offset by the increasing vertical shear. Molinari and Vollaro (1989) analyzed the outflow layer winds of Hurricane Elena (1985) during its life cycle at 12-h intervals for six days. They found that the azimuthal eddy angular momentum flux at large radii was important to the intensification of Elena. They also suggested that operational forecasts of tropical cyclones could benefit from the calculations of eddy momentum

flux because they measured the integrated effect in the storm environment, regardless of the complexity of the interactions. DeMaria et al. (1993) calculated the eddy flux convergence (EFC) of relative angular momentum for the named tropical cyclones during the 1989–91 Atlantic hurricane seasons. They found that a period of enhanced EFC within 1500 km of the storm center occurred about every 5 days due to the interaction with upper-level troughs. In addition, storms intensified just after the period of enhanced EFC in about one-third of the cases. For those cases where the storm did not intensify just after the period of enhanced EFC, either the vertical shear increased, the storm moved over cold water, or it became extratropical. They also mentioned that a statistically significant relationship (at the 95% level) was found between the EFC within 600 km of the storm center and the intensity change during the next 48 hours.

c. Influence of the environment on the outflow layer

In the past two decades, there were many observational studies (e.g. Sadler 1976, 1978; Steranka et al. 1986; Rodgers et al. 1986; Merrill 1988a,b; Molinari and Vollaro 1989, 1990; Shi et al. 1990; Rodgers et al. 1991) that linked the behavior of tropical cyclones to the strength and position of upper-tropospheric troughs and ridges (UTTs and UTRs). Sadler showed that in general as a UTT (UTR) aligns vertically with the underlying tropical cyclone, the tropical cyclone weakens (intensifies). However, the relationship between UTTs (UTRs) and tropical cyclones is not simple and straightforward. For example, Chen and Gray (1984) suggested that the outflow jets are formed by the coupling of the storm's outflow with upper- and midtropospheric troughs. Rodgers et al. (1986) also observed this phenomenon. An outflow channel to the westerlies has long been recognized as a requirement for tropical storm development. Sadler (1976) suggested that the multidirectional outflow channels to the large-scale circulation of the upper troposphere serve to remove the excess heat in the tropical cyclone's central region. Thus, a tropical cyclone is likely to intensify if it is surrounded by concentrated air currents to the east of an upper-tropospheric trough or by a strong equatorial outflow channel. Sadler (1978) further elaborated that the strengthening of an outflow channel can extend inward towards the storm center and act as a link to the cyclone's deep convection near the storm center. Holland and Merrill (1984) used observations in the Australian southwest Pacific region with an axisymmeric diagnostic model to study the dynamics of tropical cyclone structural changes. They found that a poleward outflow jet was formed by a coupling between the tropical cyclone and passing disturbances in the subtropical westerlies. They further identified that a dominant feature of the interaction was the strong poleward outflow into the divergent region ahead of an approaching westerly trough. An important conclusion of their research was that upper-tropospheric interactions between tropical cyclones and their environments can directly affect intensity change.

Recent study of satellite-measured total ozone amount by Rodgers et al. (1986) suggested that the enhancement of the inner-core convection of a tropical cyclone can be related to the upper-tropospheric environment forcing. They found that an increase in the inner-core convection in Hurricane Irene (1980) was preceded by the formation of an outflow channel. When the strength of the outflow channel decreased, the inner-core convection weakened abruptly. They also found that there was a 33-h lag between the changes in the inner-core convection and Irene's intensity changes. Based on the satellite-derived tracers (e.g., cirrus clouds, water vapor, and ozone), Rodgers et al. (1991) suggested that the intensification of Hurricane Florence was caused by the approaching of the upper-tropospheric trough from the west. They also indicated that the development of the second convective cell north of Florence's center may have been initiated by the ascending branch of the circum-jet secondary circulation at entrance region of the outflow jet of Florence enhanced by an approaching westerly UTT.

The numerical experiments by Shi et al. (1990) also showed that an accelerated outflow jet helps to increase the mass divergence in the outflow layer. Molinari and Vollaro (1989) pointed out that Hurricane Elena had a major secondary intensification associated with a large inward cyclonic eddy momentum flux produced by the passage of a middle-latitude trough north of the hurricane. Most of the past results suggest that interactions with a UTT or an upper-level westerly trough can modulate the intensification. In contrast, Merrill (1988b) argued that the environmental interactions with tropical cyclones must, in general, contribute negatively to intensity change because real tropical cyclones seldom attain the intensity allowable under theoretical constraints as described in Emanuel (1986). He asserted that interaction with an upper-level westerly trough that stimulates intensification is not apparent, because such encounters often end with tropical cyclones coming under increasing westerly shear, resulting in the filling of tropical cyclones.

The study is an attempt to substantiate the effect of interactions between tropical cyclones and UTTs in a numerical study of Hurricane Florence. The strategy is first to simulate the detailed structure of the outflow layer of Florence, and then to numerically investigate the interactions between Florence and upper-level environmental forcings. The Omega dropwindsonde (ODW)-enhanced National Meteorological Center (now the National Centers for Environmental Prediction)/Regional Analysis and Forecasting System (NMC/RAFS) 2.5° analyses (Shi et al. 1991, 1996) will be used as the initial condition for the numerical model simulations. The sensitivity of the outflow layer and the intensity of

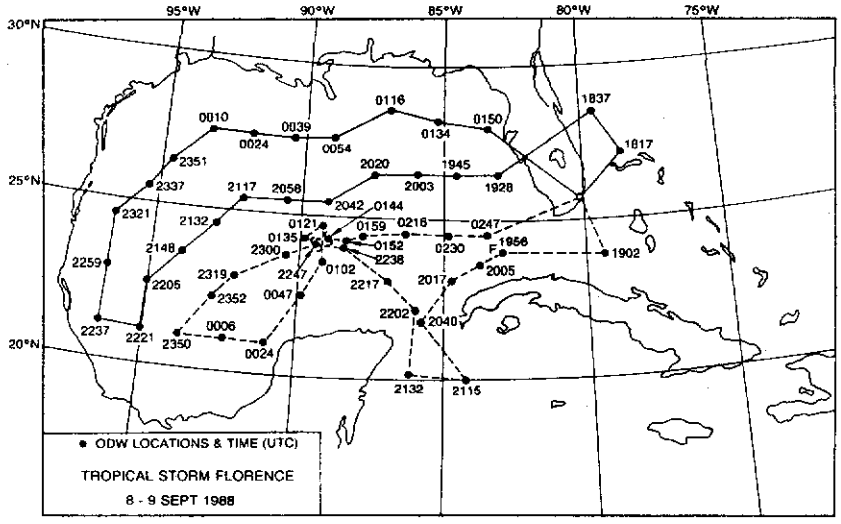

FIG. 1. Location and time (UTC) of the Omega dropwindsonde data collected during a synoptic flow experiment on 8–9 September 1988.

Florence to a westerly UTT will be examined by a series of numerical experiments.

2. Analyses

The analyses used for this numerical study were acquired from two different sources. The basic analyses were the NMC/RAFS 2.5° analyses at 0000 UTC 9 September 1988. These analyses were enhanced by the ODW data acquired from the Hurricane Research Division of the Atlantic Oceanographic and Meteorological Laboratory (AOML/HRD) of the National Oceanic and Atmospheric Administration (NOAA). Since 1982, "synoptic flow experiments" have been conducted by the AOML/HRD. The experiments are designed to determine the three-dimensional structure of tropical cyclones below ~400 mb within roughly 1000 km of the storm's center (Kaplan and Franklin 1991; Franklin et al. 1991; Franklin and DeMaria 1992). During each synoptic flow experiment, a set of ODWs were deployed from NOAA WP-3D aircraft near 400 mb over the region surrounding the targeted tropical storm.

As described in Shi et al. (1996), a total of 51 ODW data were obtained from two NOAA WP-3D aircrafts during the synoptic flow experiment on 8–9 September 1988. These data facilitate a better description of the initial condition for the numerical simulation of Florence. Figure 1 shows the two flight routes and the locations and release times of ODWs. The release times range from 1817 UTC 8 September 1988 to 0247 UTC 9 September 1988. Each ODW record consisted of the time and date of launch, location of launch (longitude and latitude), and the sounding data recorded at every 10 mb down from the flight level (ranged from 374 to 528 mb) to surface. The sounding data include pressure, temperature, relative humidity, geopotential height, wind direction, wind speed, and wind uncertainty. The wind data were missing at the lowest few levels near surface in every ODW record.

The ODW data were used to enhance the NMC/RAFS 2.5° analyses in a nested-grid analysis that will be briefly discussed in section 4. The enhanced NMC/RAFS 2.5° analyses were then used as the initial data for the numerical simulation of Hurricane Florence. The enhanced NMC/RAFS 2.5° analyses were also reprocessed in an attempt to eliminate an approaching westerly UTT coming off the Rockies to study the impact of a weaker westerly UTT on the intensification of Florence.

3. Synoptic review of Hurricane Florence (1988)

Figure 2, from Rodgers et al. (1991), shows Florence's position and intensity (maximum wind in m s^{-1}) every 6 h between 0600 UTC 7 September and 1200 UTC 10 September. Hurricane Florence's circulation started to form from a quasi-stationary frontal cloud band in the south-central Gulf of Mexico on 7 September 1988. The frontal cloud band had previously been associated with a cold front that entered the Gulf of Mexico from the northeast several days earlier. Florence was classified as a tropical depression with a maximum wind speed of 25 knots and a central pressure of 1000 mb at 0000 UTC 7 September. The circulation quickly intensified into a tropical storm with a maximum wind speed of 40 knots and a central pressure of 998 mb at 1800 UTC 7 September. It first moved eastward for 24 h and then turned northward on 8 September. It moved toward the northern Gulf Coast and became a category-1 hurricane with a maximum wind speed of 65 knots and a central pressure of 985 mb at 1800 UTC 9 September. Florence made landfall over southeastern Louisiana at 0200 UTC 10 September and quickly weakened as it

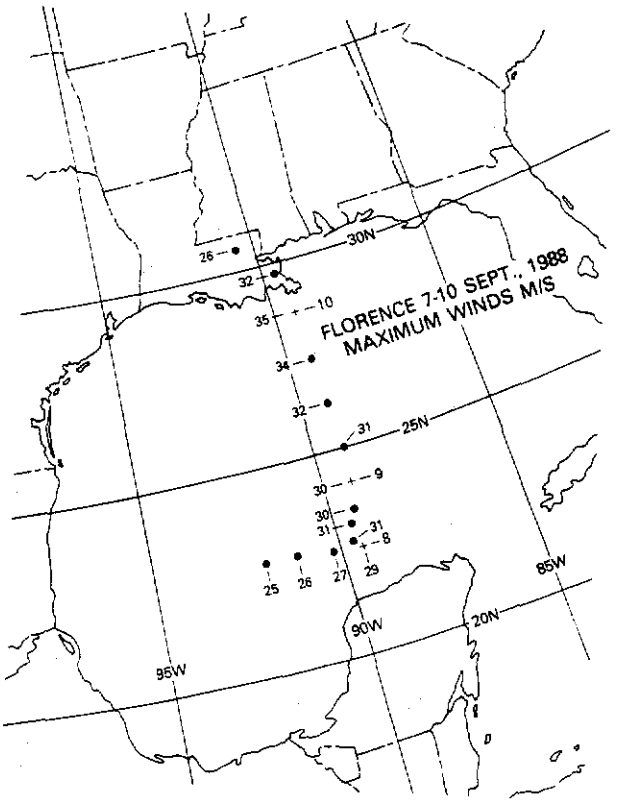

FIG. 2. Position and intensity (maximum winds in meters per second) of Hurricane Florence (7–10 September 1988) every 6 h. Crosses locate Florence's position at 0000 UTC each day. Figure adapted from Rodgers et al. (1991).

moved over the New Orleans area and dissipated on 11 September in eastern Texas (Lawrence and Gross 1989).

According to the best tracking data from the National Hurricane Center, Florence was a hurricane for only 12 h (Table 1). Air Force reconnaissance flights estimated that the highest sustained surface wind was 36 m s^{-1} and the lowest surface pressure 982 mb occurring at 2300 UTC 9 September, just 3 h before landfall. Rainfall totals of up to 100 mm were observed along the path of the storm (Lawrence and Gross 1989).

a. Evolution of Florence's precipitation and convection

Rodgers et al. (1991) presented Geostationary Operational Environmental Satellite (GOES) infrared imageries (Fig. 3) that show the development of the second deep convective cell north of the low-level center at 1200 UTC 9 September. Figure 3 shows the GOES infrared imagery every 2 h from 0200 UTC to 1200 UTC 9 September. The second deep convective cell appeared at 0800 UTC and then expeditiously expanded and intensified. At 1200 UTC, the newly developed second deep convective cell had reached a size larger than its counterpart southeast of the low-level center. Figure 3

TABLE 1. Best track of Hurricane Florence, obtained from the National Hurricane Center in Miami, Florida.

Date (d/mo)	Time (UTC)	Position: Latitude (N)	Position: Longitude (W)	Pressure (mb)	Wind (m s^{-1})	Stage
9/07	0600	22.8	92.0	1000	12.9	Tropical depression
9/07	1200	22.8	91.2	998	15.4	Tropical depression
9/07	1800	22.7	90.2	996	20.6	Tropical storm
9/08	0000	22.6	89.6	993	23.1	Tropical storm
9/08	0600	22.7	89.8	990	23.1	Tropical storm
9/08	1200	23.1	89.7	990	23.1	Tropical storm
9/08	1800	23.4	89.5	992	23.1	Tropical storm
9/09	0000	24.2	89.2	992	25.7	Tropical storm
9/09	0600	25.0	89.2	991	25.7	Tropical storm
9/09	1200	26.1	89.2	988	28.3	Tropical storm
9/09	1800	27.4	89.2	985	33.4	Hurricane
9/10	0000	28.7	89.3	983	36.0	Hurricane
9/10	0600	29.7	89.7	988	30.9	Tropical storm
9/10	1200	30.7	90.7	998	15.4	Tropical depression
9/10	1800	31.8	91.5	1003	10.3	Tropical depression
9/11	0000	32.4	92.3	1007	7.7	Tropical depression
9/11	0600	32.7	93.3	1009	7.7	Tropical depression
9/11	1200	33.0	94.5	1010	7.7	Tropical depression
9/09	2300	28.5	89.3	982	36.0	Minimum pressure
9/10	0200	29.1	89.3	984	36.0	Landfall

also confirms the existence of a large rain band that stretched from the convective region to the area off the east coast of the Yucatan Peninsula. The Special Sensing Microwave/Imager (SSM/I) precipitation rates at the same time (Fig. 4) also reveal the development of the second deep convective cell north of the low-level center. The second convective cell eventually merged with the convection to the southeast of the low-level center and the combined convective region moved northward toward New Orleans.

b. Upper-tropospheric environment of Florence and its possible influences on Florence's outflow

Before Florence became a hurricane on 9 September, there was a westerly UTT approaching from the west as shown in the NMC/RAFS 2.5° analysis at 1200 UTC 8 September (Fig. 5). The trough extended from the southern part of Illinois into the eastern part of Texas. Twelve hours later, at 0000 UTC 9 September, the UTT moved eastward into the northern Gulf of Mexico, originating from Tennessee (Fig. 6). At this time, the westerly jet (Fig. 6) might have provided a channel for the forming of the outflow jet of Florence and initiated the development of the second convective cell north of Florence's center a few hours later, as described in the previous section. At 1200 UTC 9 September, the UTT (Fig. 7) moved slightly eastward and was apparently weakening as compared to the UTT in Fig. 6. During the next 12 h, the westerly jet had moved northward, judging from the shaded area representing the wind speed of 30 m s^{-1} and greater in Fig. 8. Florence had also moved under the UTT in its continuous northward

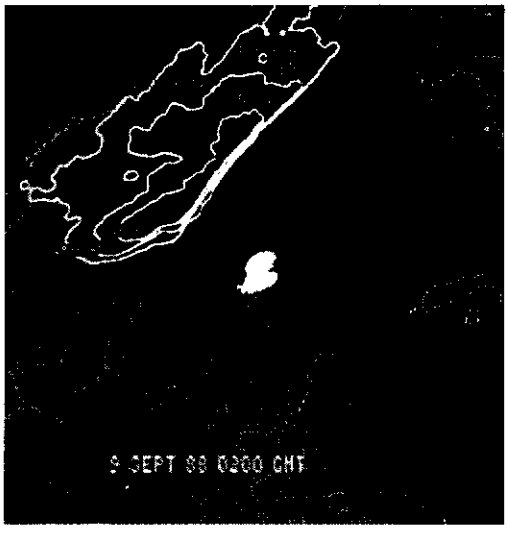
9 SEPT 68 0200 GMT

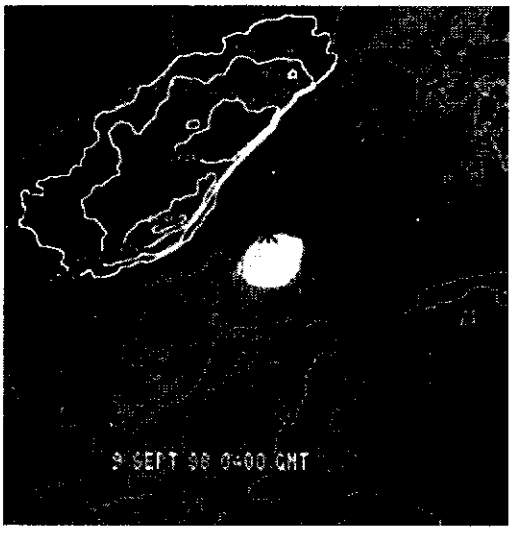
9 SEPT 68 0400 GMT

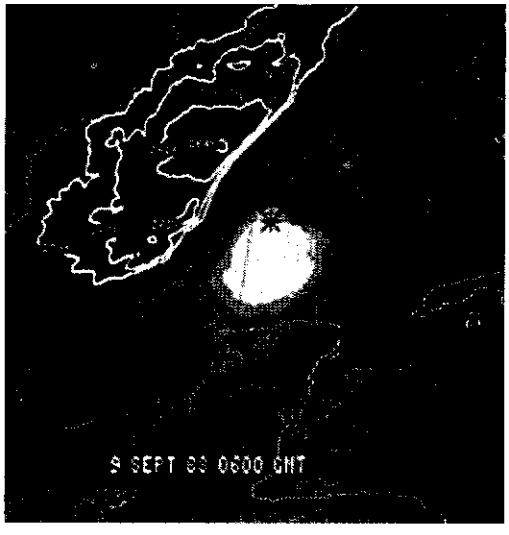
9 SEPT 68 0600 GMT

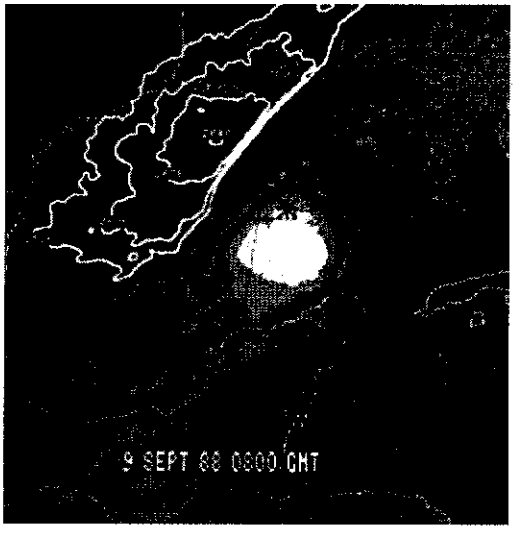
9 SEPT 68 0800 GMT

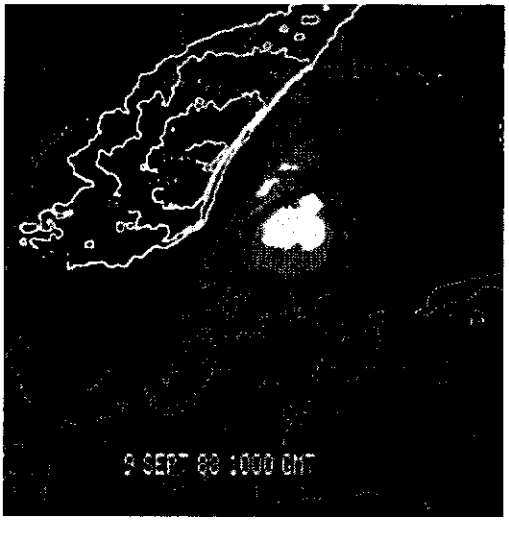
9 SEPT 68 1000 GMT

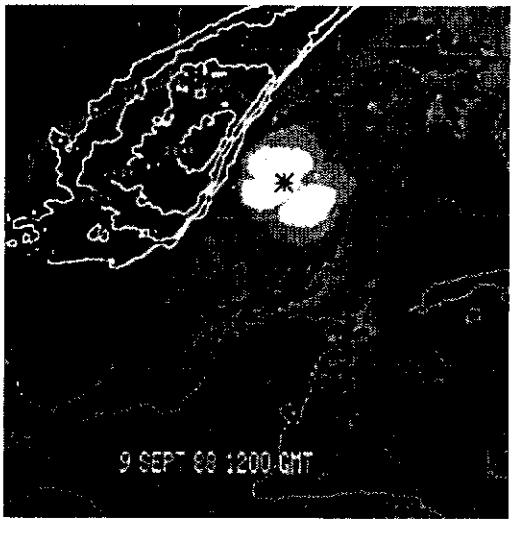
9 SEPT 68 1200 GMT

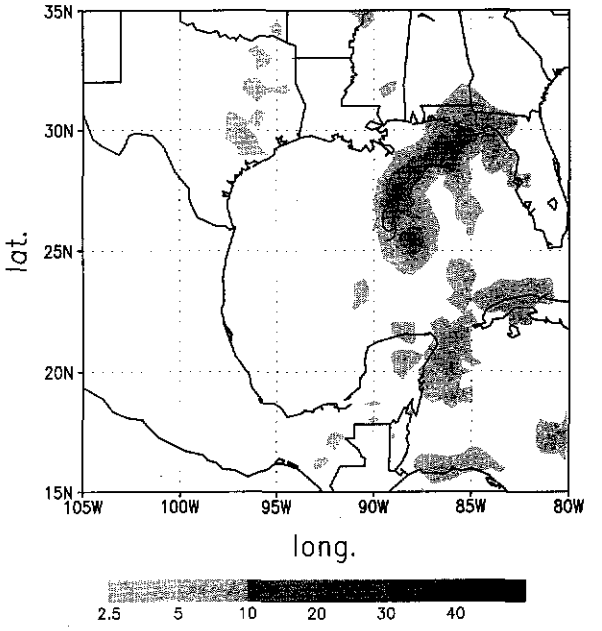

FIG. 4. SSM/I-retrieved rain rates at 1200 UTC 9 September 1988.

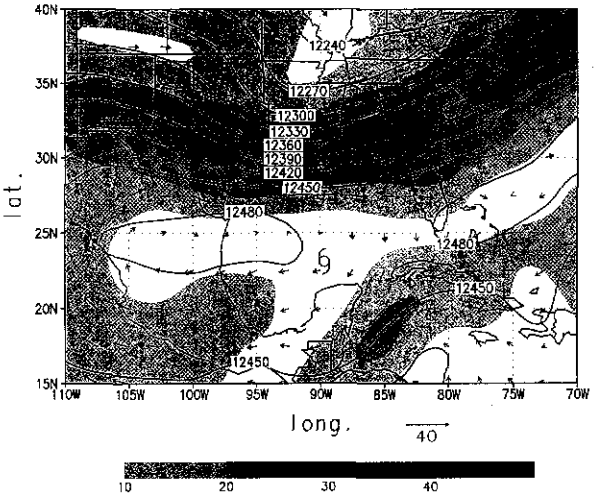

FIG. 5. 200-mb geopotential height contours (m), wind vectors, and shaded isotachs (m s^{-1}) of the NMC/RAFS 2.5° analysis at 1200 UTC 8 September 1988. The hurricane symbol depicts the current center location of Florence from the best track record.

movement. The increasing vertical shear probably had become a negative factor of Florence's further intensification. At this time, Florence was also about to make landfall.

Rodgers et al. (1991) used satellite-derived cirrus-level winds to show the approaching of the UTT from the west. Figure 9 shows the cirrus-level streamline analyses and wind speeds at 12-h interval from 1200 UTC 8 September to 1200 UTC 9 September. At 1200 UTC 8 September (Fig. 9a), there was a UTT in the northwestern Gulf of Mexico just northwest of Florence's center. Twelve hours later (Fig. 9b), the UTT became deeper and stronger and extended further south as Florence moved northward. Figure 9c shows the development of the outflow jet located north of Florence's center at 1200 UTC 9 September, suggesting that Florence's northern outflow became channeled and enhanced as the system interacted with the UTT. Rodgers et al. (1991) speculated that the combination of the observed evolution of Florence's outflow (Fig. 9) and the convection (Figs. 3 and 4) provides some evidence that the outflow jet-induced secondary circulation might enhance the convective growth in the entrance region of the outflow jet. The mechanism was also illustrated in the numerical study of Shi et al. (1990) using an idealized tropical cyclone.

4. Numerical model and experimental design

The Naval Research Laboratory's limited-area numerical prediction system, a research version of the Navy Operational Regional Atmospheric Prediction System, was used in this study. The system includes a data assimilation system, a vertical mode initialization (VMI), and a limited-area numerical model. The data assimilation system includes two steps. The first step is a data preparation and quality control scheme and the second step is an objective analysis scheme. The data quality control consists of a "gross" check and a "buddy" check following DiMego (1988). The objective analysis is a three-pass nested-grid Barnes scheme (Shi et al. 1991, 1996). The VMI, as described in Sashegyi and Madala (1993), produces a balanced vertical motion field and induces smaller changes to the initial mass and wind fields as compared to static initialization schemes.

The limited-area numerical model is a three-dimensional, hydrostatic, primitive equation model incorporating a split-explicit time integration scheme (Madala 1981). Details of the model are described in Madala et al. (1987), Chang et al. (1989), and Holt et al. (1990). However, in this version of the model, there are 23 layers in the vertical direction. A terrain following σ ($=P/P_s$) vertical coordinate and time-dependent lateral boundary conditions are utilized, where P is the pressure and P_s the surface pressure. Topography used in this model is derived from the U.S. Navy global 10-minute elevation

←

FIG. 3. GOES Visible and Infrared Spin Scan Radiometer (VISSR) infrared (11.5 mm) image of Hurricane Florence between 0200 UTC and 1200 UTC 9 September 1988 at 2-h intervals. The white contours depict the warmest VISSR infrared water vapor (6.7 mm) brightness temperature between 258° and 264 K at 2-K intervals. The star depicts Florence's center. Figure adapted from Rodgers et al. (1991).

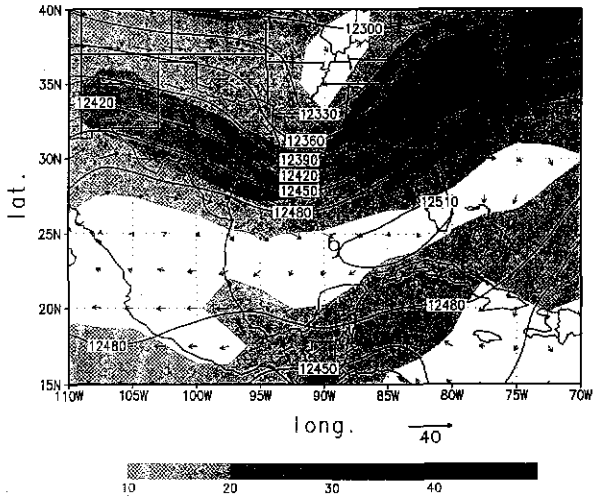

FIG. 6. Same as Fig. 5 except for 0000 UTC 9 September 1988.

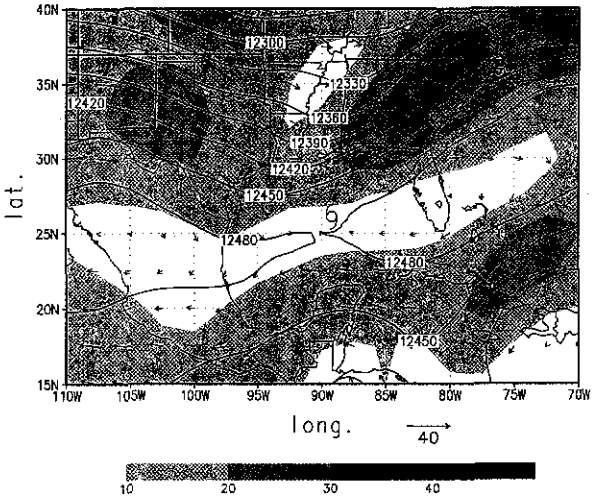

FIG. 7. Same as Fig. 5 except for 1200 UTC 9 September 1988.

data. The grid domain, from 15° to 45°N and from 110° to 65°W, covers most of the continental United States and all of the Gulf of Mexico, with horizontal resolutions of one-half and one-third degree in longitude and latitude, respectively. The main interest of this study is in the upper layer, which contains synoptic or larger scale phenomenon. Therefore, the horizontal resolution is appropriate for this study.

The planetary boundary layer parameterization of this model is based on the two-parameter formulation of Detering and Etling (1985) as described in Holt et al. (1990). Temperature at the lowest model layer (σ = 9.9975) at the initial time is used as ground temperature. The sea surface temperature is obtained from the multichannel sea surface temperature (MCSST) data derived from Advanced Very High Resolution Radiometer imageries. This MCSST product is a weekly composite for the global SST at a horizontal resolution of approximately 18 km. The model uses a modified Kuo scheme for parameterizing the effect of cumulus convection (Kuo 1965; Anthes 1977). The large-scale precipitation occurs when there is a supersaturated layer in the model.

The ODW data were used to enhance the NMC/RAFS 2.5° analyses by using the three-pass nested-grid Barnes scheme. The horizontal resolution in the first two passes is one-half degree and one-sixth degree in the third pass. The selection of the different resolutions for the different passes in the objective analysis matches the ODW data resolutions (Fig. 1). As shown in Fig. 1, it is apparent that the ODW data resolution near Florence's center is about three times higher than the ODW data resolution away from Florence's center. Details of the analysis of the ODW data are described in Shi et al. (1991, 1996). The enhanced analyses were initialized by the VMI and used as the initial data of the model integration for the different numerical experiments. In this study, the limited-area model was integrated with the ODW-enhanced analyses at 0000 UTC on 9 September 1988 for 48 h (Expt. ODW). Details of the intensity and track simulation results were documented in Shi et al. (1996).

5. Simulated structure of the outflow layer of Hurricane Florence

a. Simulated outflow structure at 200-mb level

Figure 10 shows the simulated 200-mb geopotential heights, wind vectors, and isotachs of Expt. ODW at 12 h valid at 1200 UTC 9 September. There is a westerly trough extending from western Tennessee to Louisiana and the northern Gulf of Mexico, agreeing with the NMC/RAFS 2.5° analysis at 1200 UTC 9 September (Fig. 7). There is an upper-level high pressure located near the center of the Gulf of Mexico, corresponding to the low-level center of Florence. The outflow layer is highly asymmetric, especially beyond three degrees

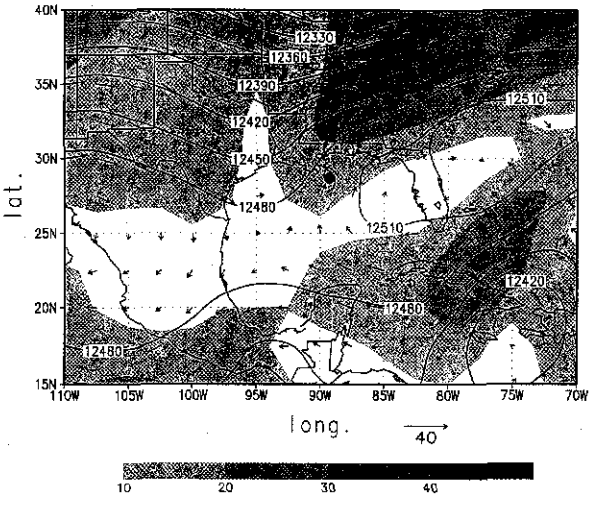

FIG. 8. Same as Fig. 5 except for 0000 UTC 10 September 1988.

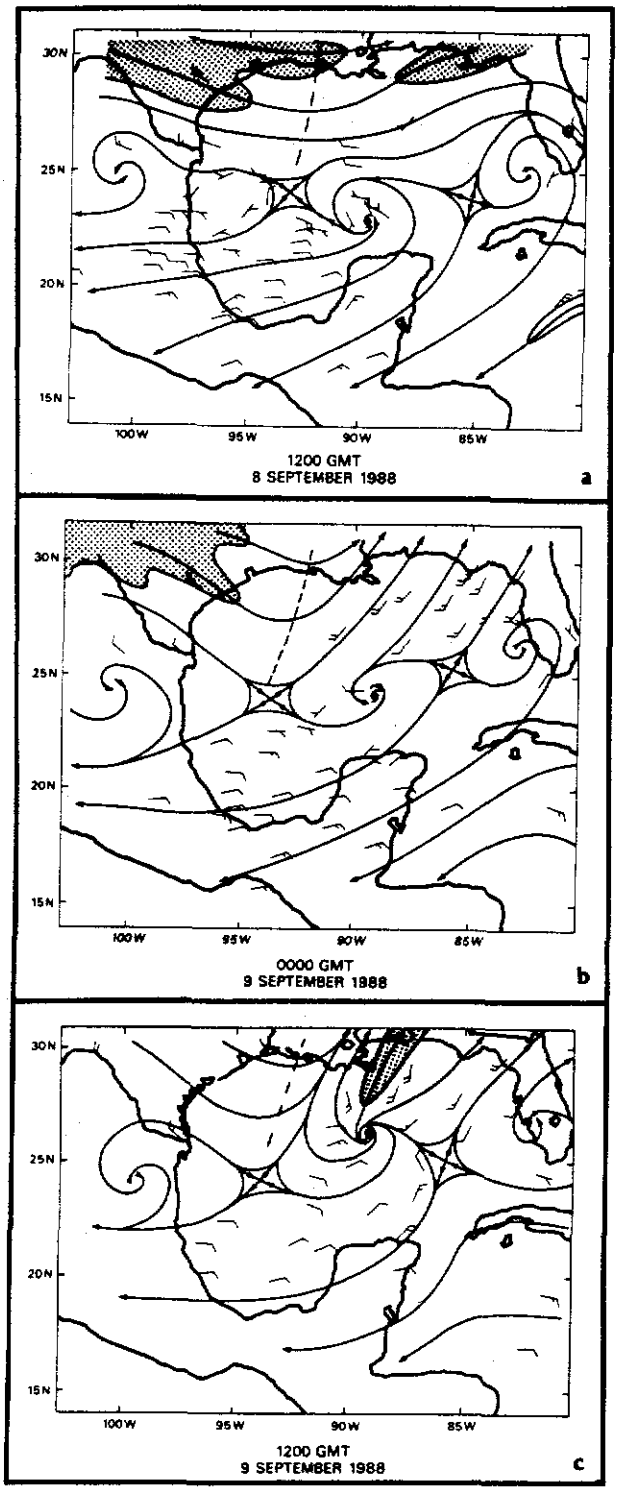

FIG. 9. Cirrus-level winds (m s^{-1}) and streamline analysis for Hurricane Florence at (a) 1200 UTC 8 September, (b) 0000 UTC, and (c) 1200 UTC 9 September 1988. Shaded area represents wind speeds $\geq$25 m s^{-1}. Hurricane symbol depicts the center of Florence. Dashed line represents the upper-level tropospheric trough's axis. Full wind barb represents 10 m s^{-1}. Figure adapted from Rodgers et al. (1991).

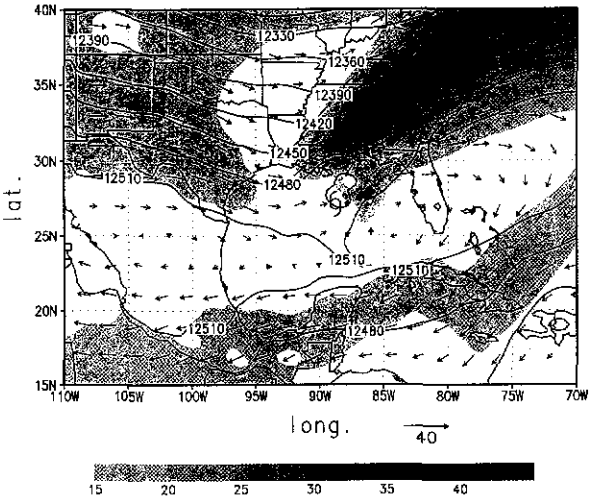

FIG. 10. 200-mb geopotential heights, wind vectors, and shaded isotachs (m s^{-1}) of Expt. ODW at 12 h valid at 1200 UTC 9 September 1988. The hurriccane symbol depicts the current center location of the simulated Florence.

radius, with an outflow channel or jet starting from about three degrees north of the center and extending northeastward into the mid-Atlantic states and Atlantic Ocean. The outflow jet is elongated with a length of roughly 2500 km and a width of 500 km as outlined by the shaded area of 30 m s^{-1} and greater (Fig. 10). The location of the outflow jet also agrees with NMC/RAFS 2.5° analysis at 1200 UTC 9 September (Fig. 7), except the simulated jet is stronger, better defined, and better connected with Florence. The simulated outflow jet has a maximum wind speed of 42.4 m s^{-1}, which is 5.8 m s^{-1} stronger than the one in the NMC/RAFS 2.5° analysis. It also shows an anticyclonic curvature. As shown in Fig. 10, at the entrance region of the jet (near the Louisiana, Mississippi, and Alabama coasts), there is a strong anticyclonic (cyclonic) shear along the southeastern (northwestern) edge of the jet core. Downstream at the exit region, the jet becomes diffused with diminishing horizontal shears at both sides of the jet. These characteristics of the outflow jet are similar to those in the idealized model by Shi et al. (1991). At 24 h valid at 0000 UTC 10 September, the 200-mb geopotential heights, wind vectors, and isotachs (Fig. 11) show that the westerly jet has moved northeastward over Virginia and becomes disassociated with Florence. Florence's center has also moved northward and into a region under the south end of the westerly trough. Increase of the mean 200–850-mb vertical wind shear in a 5° × 5° box centered at storm center from 9.5 m s^{-1} at 12 h to 14.3 m s^{-1} at 24 h probably prevented Florence from any further intensification. At this time, Florence is also about to make landfall, and its behavior will be dominated by the response to the landfall.

The structure of the relative humidity (RH) field at upper levels is usually determined by the three-dimen-

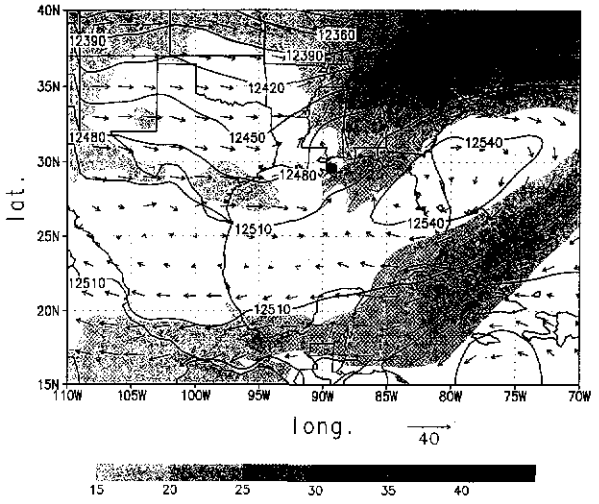

FIG. 11. Same as Fig. 10 except for at 24 h valid at 0000 UTC 10 September 1988.

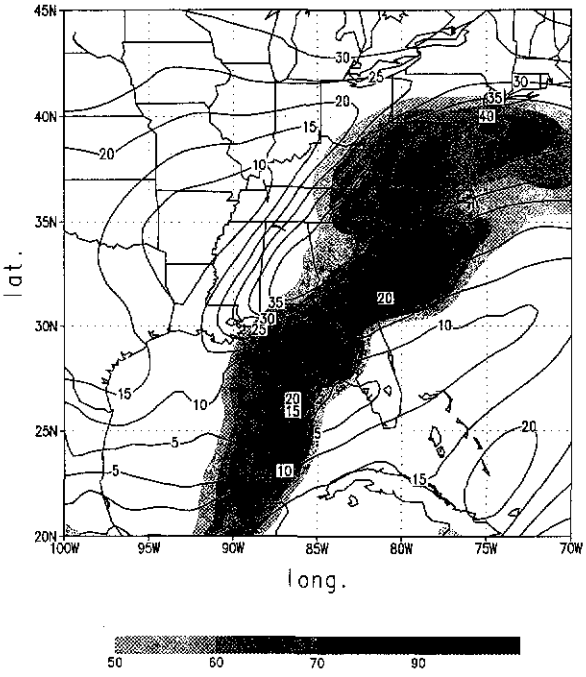

FIG. 12. 200-mb relative humidities (%) (shaded area) and isotachs (contour) of Expt. ODW at 12 h valid at 1200 UTC 9 September 1988.

sional transport process in the outflow layer, reflecting the important features of the outflow momentum field. Figure 12 shows the 200-mb RH in the outflow layer at 12 h. There is a wet canopy with RH > 90% over the storm center, which also extends northeastward along the anticyclonic shear side of the outflow jet. The moisture field is clearly asymmetric relative to the jet core with high RH (>90%) on the anticyclonic shear side of the outflow jet from the Florida panhandle to the South Carolina coast and low RH (<50%) on the cyclonic shear side of the jet located to the northwest of the jet. This particular RH distribution suggests that there is a circum-jet secondary circulation with ascending motion on the anticyclonic shear side and descending motion on the cyclonic shear side as discussed in Shi et al. (1990). Further downwind from the jet core, a high RH region (>90%) is located over Virginia, and there is a dry wedge (RH < 60%) located over Cape Hatteras, North Carolina. The dry wedge located downstream from the high RH cannot be the result of the horizontal transport and therefore must be caused by vertical motions at this level. The moisture field, characterized by the alternate dry and wet regions on either side of the outflow jet, is an indication of the existence of the thermally direct (indirect) secondary circulation in the entrance (exit) region of the outflow jet found in an idealized tropical cyclone (Shi et al. 1990).

b. Cross sections of the simulated outflow jet

To further illustrate the secondary circulations, we examine the cross-sectional structure of the wind and moisture fields. A composite cross-sectional structure of the wind and RH field is obtained by averaging the values of the cross-sections of the outflow jet. The composite cross section representing the entrance region of the outflow jet is an average of seven cross sections as indicated in Fig. 13. In the exit region, six cross sections are computed and averaged.

Figure 14 shows the composite cross section of the wind and RH field in the entrance region at 12 h valid at 1200 UTC 9 September. The vectors are formed by the vertical velocities (in mb h^{-1}) and horizontal wind

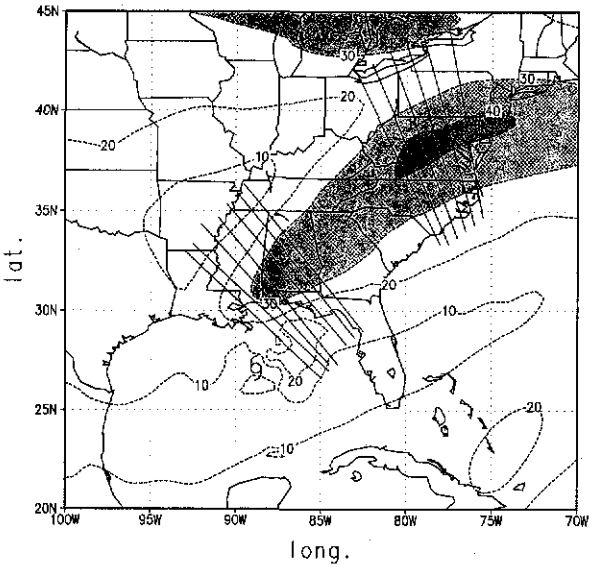

FIG. 13. Location of cross sections. Seven cross sections are in the entrance region of the outflow jet, and six cross sections are in the exit region. Contours are the 200-mb isotachs. Shaded area represents the area with wind speed greater than 30 m s^{-1}.

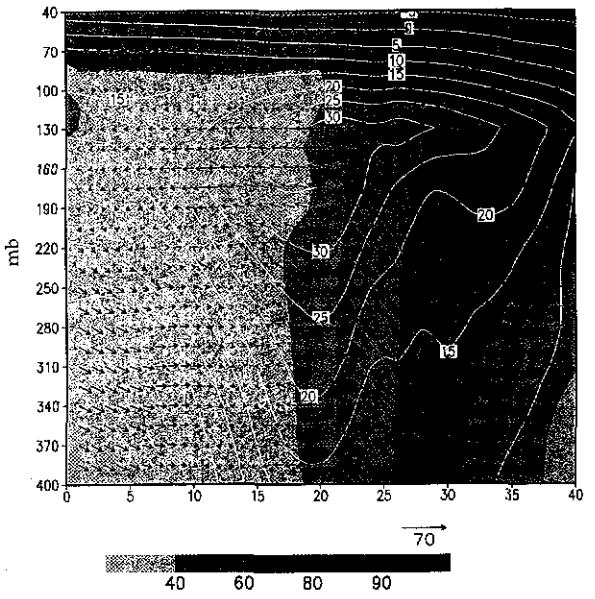

FIG. 14. Composite cross section in the entrance region of the outflow jet of Expt. ODW at 12 h. The orientation of the cross section is looking downwind along the outflow jet with approximately NW to the left and SE to the right. Contours are the wind component (m s^{-1}) normal to the cross section (positive means blowing into the paper). Vectors are the combination of the vertical velocity (mb h^{-1}) and the wind component (m s^{-1}) tangential to the cross section. Shaded area are the relative humidity (%).

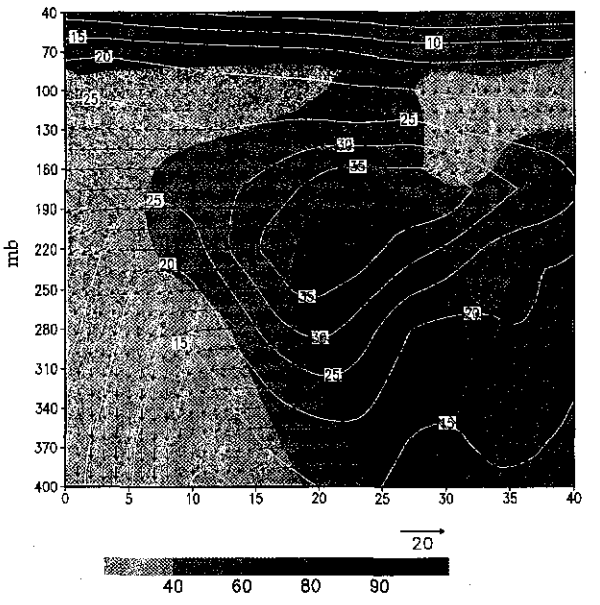

FIG. 15. Same as Fig. 14 except for the composite cross section in the exit region of the outflow jet.

components (in m s^{-1}) tangential to the cross section. The isotachs are the horizontal wind components (m s^{-1}) normal to the cross section with positive values for the southwesterly wind (into the cross section). In the jet entrance region (Fig. 14), the high RH (>90%) is located on the anticyclonic shear side of the outflow jet, coinciding with a strong ascending motion, while the low RH (<50%) is on the cyclonic shear side coinciding with a weak descending motion. There is an abrupt, vertically aligned RH gradient at the jet core. There is also an outward (from the anticyclonic to cyclonic shear side of the outflow jet), cross-jet mean horizontal motion between 130 and 250 mb. Merrill (1984) and Shi et al. (1990) suggested that the circum-jet secondary circulation has an outward branch above the jet, an inward branch below the jet (near 400 mb), an ascending branch on the anticyclonic shear side, and a descending branch on the cyclonic shear side of the outflow jet. The result shown here also indicates the existence of the circum-jet secondary circulation in the outflow layer. The inward branch below the outflow jet in the entrance region is, however, less apparent in this study, probably due to the presence of the coastal warm front and other synoptic features. In this real case study, it is difficult to clearly separate the secondary circulations associated with the outflow jet and vertical motions that are associated with other synoptic systems.

Figure 15 shows the composite cross section in the exit region. The jet core has descended from 130–220 mb in the entrance region to 145–280 mb in the exit region. Here, the moisture field on the cyclonic shear side has become more humid, and the anticyclonic shear side has become drier (<60%) between 100 and 190 mb compared to their counterpart in the entrance region (Fig. 14). Comparing Figs. 14 and 15, the high RHs in the jet have moved outward and downward downstream, consistent with the reversal of the secondary circulation. In addition, there appears to be a northwestward tilt of the high RH region, which may be related to the pre-existing coastal front along the mid-Atlantic coast. As shown in Fig. 15, there is a thermally indirect secondary circulation between 100 and 190 mb with an ascending motion on the cyclonic shear side and a descending motion on the anticyclonic shear side. The drier region on the anticyclonic shear side coincides with the descending branch of the secondary circulation. The outward branch moves through the jet core, and the inward branch is situated just above the jet.

c. *Angular momentum budget*

Previous studies (Black and Anthes 1971; Holland 1983; Molinari and Vollaro 1989; DeMaria et al. 1993) showed that the inward azimuthal eddy cyclonic angular momentum flux (AMF) is important to the intensification of tropical cyclones. Challa and Pfeffer (1990) claimed that the characteristic difference between the developing and nondeveloping disturbances is the presence (in the developing disturbances) of the well-developed influx of cyclonic eddy angular momentum at outer radii in the upper troposphere. Molinari and Vollaro (1989) studied the interaction between Hurricane Elena (1985) and its upper-tropospheric environment

TABLE 2. Model and empirical angular momentum budget in the outflow layer of tropical cyclone. Units are in 10^{22} g cm^2 s^{-2}. The values for mean storms are adopted from Anthes (1974). The values from the current study are storm relative.

	Radius (km)	Coriolis torque	Horizontal flux		Vertical flux	
			Mean	Eddy	Mean	Eddy
Mean storm (Palmen and Riehl 1957)	0–333	−48.0	−20.0	8.0	40.0	20.0
	333–666	−143.0	76.0	23.0	—	44.0
Mean storm (Pfeffer 1958)	222–444	−54.0	46.0	20.0	5.0	—
	444–666	−78.0	−11.0	13.0	−4.0	—
Model storm (Shi et al. 1990)	0–300	−4.3	3.5	−0.7	−0.3	—
	300–1000	−47.6	13.4	35.1	1.1	−0.4
Model Florence (1988) from Expt. ODW	0–300	−8.4	5.3	−3.5	−1.8	−1.2
	300–700	−99.2	49.6	30.6	0.9	1.4
Model Florence (1988) from Expt. ODW + WTR	0–300	−8.9	5.9	−2.3	−2.8	−0.7
	300–700	−104.3	55.6	25.0	−0.6	0.3

and concluded the AMF measures the integrated effects of the interactions between the tropical cyclones and their environments, regardless of the complexity of the interactions.

The budget of the angular momentum of the outflow layer is calculated to study the importance of the eddy AMF. Following Anthes (1974) and Shi et al. (1990), the angular momentum budget equation in a cylindrical coordinate system is defined as

$$\frac{\partial M}{\partial t} = -2\pi \int_{h_1}^{h_2} \int_{r_0}^{r_1} r^2 \rho(z)(\langle f \rangle \langle u \rangle + \langle f'u' \rangle)\, dr\, dz$$
$$-2\pi \int_{h_1}^{h_2} [r_1 \rho(z)(\langle m \rangle \langle u \rangle)_{r_1} - r_0 \rho(z)(\langle m \rangle \langle u \rangle)_{r_0}]\, dz$$
$$-2\pi \int_{h_1}^{h_2} [r_1 \rho(z)(\langle m'u' \rangle)_{r_1} - r_0 \rho(z)(\langle m'u' \rangle)_{r_0}]\, dz$$
$$-2\pi \int_{r_0}^{r_1} r[(\rho \langle w \rangle \langle m \rangle)_{h_2} - (\rho \langle w \rangle \langle m \rangle)_{h_1}]\, dr$$
$$-2\pi \int_{r_0}^{r_1} r[(\rho \langle m'w' \rangle)_{h_2} - (\rho \langle m'w' \rangle)_{h_1}]\, dr, \qquad (1)$$

and

$$M = \int_{h_1}^{h_2} \int_{r_0}^{r_1} \int_0^{2\pi} r\rho m\, d\lambda\, dr\, dz, \qquad (2)$$

where $m = rv$ (relative angular momentum); u and v are the radial and tangential velocities in storm-relative cylindrical coordinates, (λ, r, z) respectively; and r is the radius from the storm center as determined by the sea level pressure (SLP). In Eq. (1), the symbol $\langle\ \rangle$ represents an azimuthal mean and $(\ )'$ denotes a deviation from the mean. Vertical integrations are carried out between the geopotential heights of $h_1 = 13\,500$ gpm and $h_2 = 14\,500$ gpm, containing most of the outflow. The first terms on the right-hand side of Eq. (1) denotes the mean and eddy Coriolis torques and the second and third terms denote the horizontal convergence of mean and eddy angular momentum fluxes, respectively. Finally, the fourth and fifth terms represent the vertical convergence of mean and eddy angular momentum fluxes, respectively. To evaluate these terms, model results are linearly interpolated to the cylindrical coordinates. Because of the size of Florence, the outer region is defined from 300 to 700 km, instead of the 300 to 1000 km used in Shi et al. (1990). The values of each term in Eq. (1) calculated from Expt. ODW's result at 12 h are listed in Table 2. For comparison, values from the idealized model tropical cyclone in Shi et al. (1990) and observed values for mean tropical storms in Palmen and Riehl (1957), as well as in Pfeffer (1958), are also listed.

Table 2 shows that the values of various terms in Eq. (1) evaluated from the modeled tropical cyclones compare reasonably with those of the observational studies and the previous model study. The vertical momentum fluxes in Palmen and Riehl (1957) contained unaccounted-for residuals. In general, the angular momentum balance in both the simulated and the observed tropical cyclones is basically maintained by the Coriolis torque and horizontal transports, especially at outer radii where the vertical transport is small. The values in Table 2 suggest that the mean horizontal AMF dominates in the inner region, while the eddy horizontal AMF is roughly equal to the contribution from the mean in the outer region. The large positive eddy horizontal AMF at large radii, meaning a large inward cyclonic eddy momentum flux, agrees with the observational study of Molinari and Vollaro (1989). All budget calculations indicate the importance of the eddy horizontal AMF for the angular momentum balance in the outer region. Results from the model storm of Shi et al. (1990) and Expt. ODW show a negative contribution of the horizontal eddy AMF in the inner region, reflecting the cyclonic circulation near the storm center in the outflow layer. The important role of the eddy momentum transport in the angular momentum budget underscores the dominance of the outflow jet in the outflow layer of the tropical cyclone, in this case, Hurricane Florence. Results from Expt. ODW+WTR will be discussed in the next section.

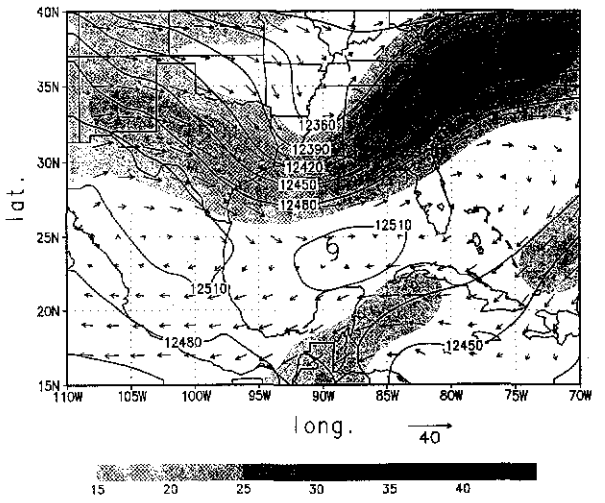

FIG. 16. 200-mb geopotential heights (m), wind vectors, and shaded isotaches (m s^{-1}) of the ODW enhanced analyses after initialized by the VMI. The hurricane symbol depicts the current center location of Florence from the best track record.

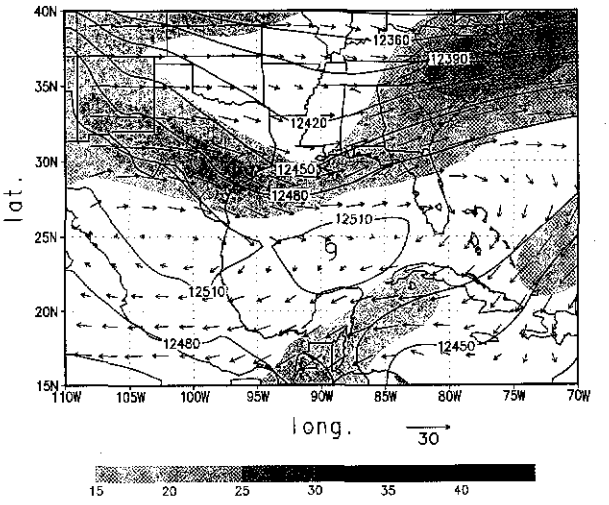

FIG. 17. Same as Fig. 16 except for the reprocessed ODW-enhanced analysis.

6. Upper-tropospheric environmental influences on Florence

To further isolate the cause–effect relationship between the upper-tropospheric trough and intensity and structural changes of Hurricane Florence, a numerical experiment (Expt. ODW+WTR) is conducted for this study. For this experiment, the ODW-enhanced analyses are reprocessed to reduce the cyclonic curvature of the upper-level westerly trough at 0000 UTC 9 September. This is done to determine the impact of the weakened westerly jet on the outflow layer of Florence. In the reprocessed version of the ODW enhanced analyses, the north–south component of the wind is set to zero in the layer between 100 and 500 mb and in the region between 30° and 45°N. To further weaken the temperature gradient associated with the westerly jet, the temperature at each grid point in the same region is set to the zonal mean temperature. The reprocessed data are then initialized by the VMI. Comparing Fig. 16 and 17, the amplitude of the upper-level westerly trough is apparently weakened by the reprocess, with the maximum wind speed in the upper-level westerly jet reduced by 4.9 m s^{-1} from 34.5 m s^{-1} to 29.6 m s^{-1}, a reduction of ~14%. The tropical cyclone model is then integrated for 48 h with the reprocessed analyses to simulate the would-be behavior of Florence under the influence of a weakened westerly jet.

As shown in Fig. 18, the minimum SLP of Expt. ODW+WTR at 24 h is 2 mb weaker than the one of Expt. ODW, and the maximum surface wind of Expt. ODW+WTR is 5.0 m s^{-1} or 13% weaker than that of Expt. ODW. A weaker westerly trough and jet result in a weaker intensification of Florence. Figure 19 shows the simulated 200-mb geopotential heights, wind vectors, and isotaches of Expt. ODW+WTR at 12 h. It is apparent that the maximum wind in the outflow jet of Expt. ODW+WTR is 6.4 m s^{-1} or ~15% weaker than that of Expt. ODW (Fig. 10). The comparison suggests that the intensification of Florence is very much correlated to the approaching westerly jet.

Previous studies (Holland and Merrill 1984; Merrill 1984; Shi et al. 1990) suggested that the outflow jet provides a channel to remove the warm air from the core of tropical cyclones, and as a result, the convection in the core region can be enhanced. Figure 20 shows that the mean convective precipitation of Expt. ODW + WTR inside a 2° × 2° box centered at the storm center is reduced by about an average of 15–20% between 10 and 15 h, coinciding with the 15% reduction of the maximum wind in the outflow jet. The weaker convection in the core region between 10 and 15 h eventually results in a weaker hurricane at 24 h. These results are consistent with Holland and Merrill (1984) and Shi et al. (1990). Figure 20 also shows that the inner core convection of Expt. ODW and ODW+WTR reach their maximum at 13 h, while the intensities of both storms reach their maximum at 23 h, suggesting a 10-h lag between the maximum convection and the maximum intensity in Florence.

Figure 21 shows the 12-h 200-mb RH field of Expt. ODW+WTR. Similar to the 12-h 200-mb RH contours of Expt. ODW (Fig. 12), the moisture field features a wet region (RH > 90%) on the anticyclonic shear side of the jet, indicating the existence of the secondary circulation. The broader wet region is a consequence of a broader secondary circulation in this experiment. However, the secondary wet region, embedded in the cyclonic shear side of the exit region of the jet of Expt. ODW over Virginia (Fig. 12), is conspicuously absent in Expt. ODW+WTR, indicating a weaker outflow, a weaker and broader thermally direct circulation, and the

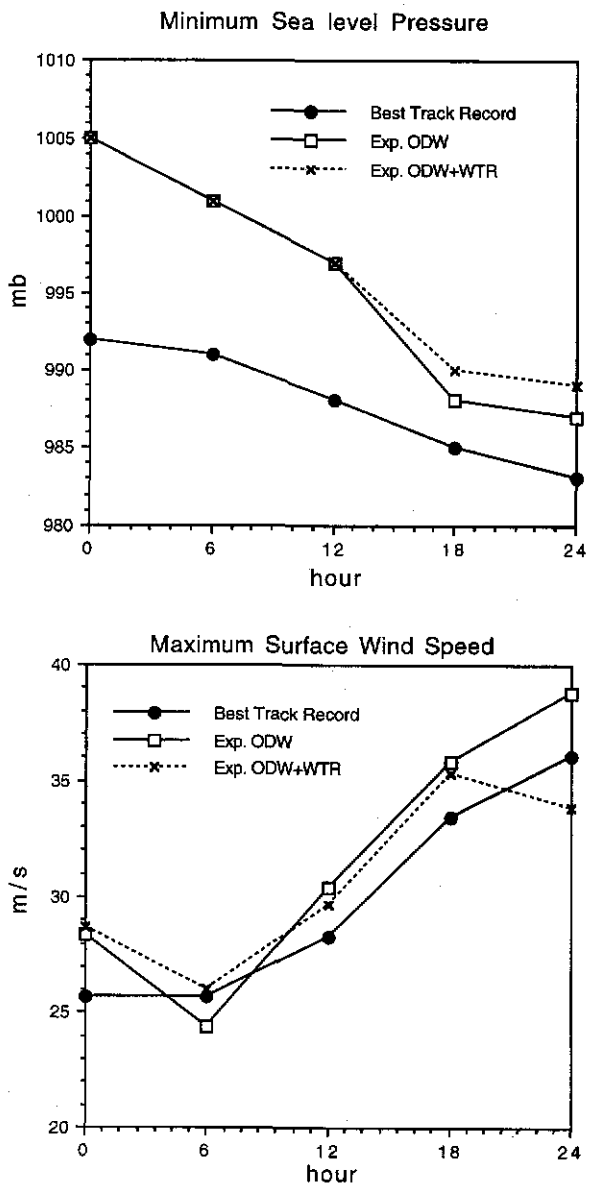

FIG. 18. Time variation of the minimum sea level pressure (mb) and maximum surface wind speed (m s^{-1}) of Expt. ODW and ODW+WTR.

absence of the thermally indirect circulation because of a weaker approaching westerly UTT.

Table 2 also lists the storm-relative angular momentum budgets calculated from Expt. ODW+WTR's result at 12 h using Eq. (1). The result shows a larger (smaller) net horizontal import of the eddy (mean) cyclonic angular momentum corresponding to a stronger outflow jet of Expt. ODW as compared to a smaller net horizontal eddy import in Expt. ODW+WTR at large radii. This result indicates that the outflow jet and the eddy import of cyclonic angular momentum are stronger with a stronger approaching westerly UTT, consistent with Challa and Pfeffer (1990). Further evidence of the influence by the approaching westerly UTT can be seen in the change of storm-relative, horizontal eddy AMF (Fig. 22). In both experiments, Florence experienced an increase of horizontal import of eddy cyclonic angular momentum before 15 h. In Expt. ODW, the stronger approaching westerly UTT is correlated with a larger increase of eddy convergence flux and more intense inner core convection (Fig. 20) before 15 h. Eddy heat fluxes in the upper troposphere are also calculated. Results show that a cooling of 4 K day^{-1} by eddies exists at radius between 400 and 700 km between 15 and 18 h in Expt. ODW, up from 2 K day^{-1} at 12 h. In contrast,

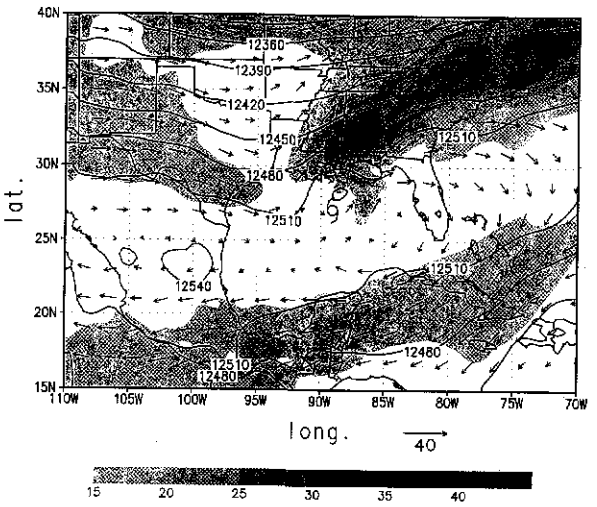

FIG. 19. Same as Fig. 10 except for Expt. ODW+WTR at 12 h.

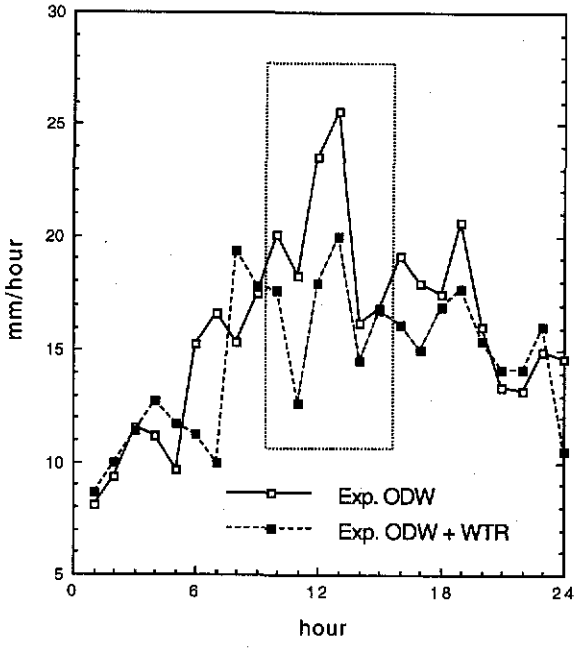

FIG. 20. Mean convective rain rates of Expt. ODW and ODW+WTR inside a 2° × 2° box centered at the storm center. Dashed box contains mean convective rain rates between 10 and 15 h.

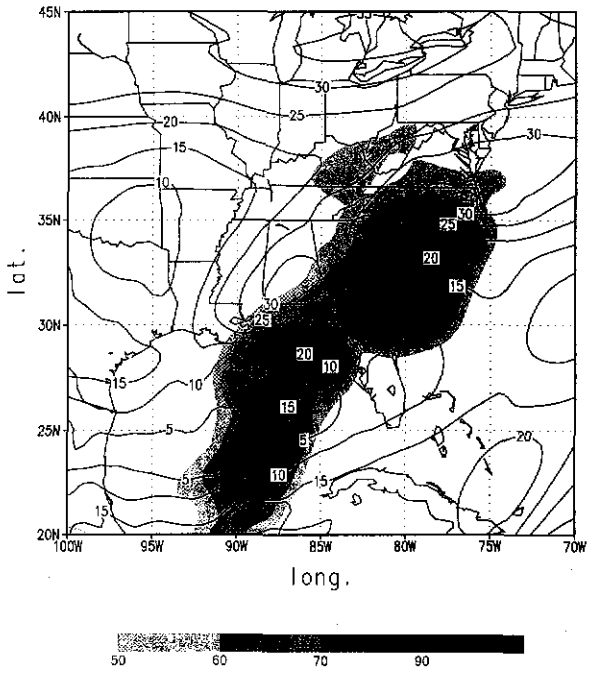

FIG. 21. Same as Fig. 12 except for Expt. ODW+WTR at 12 h.

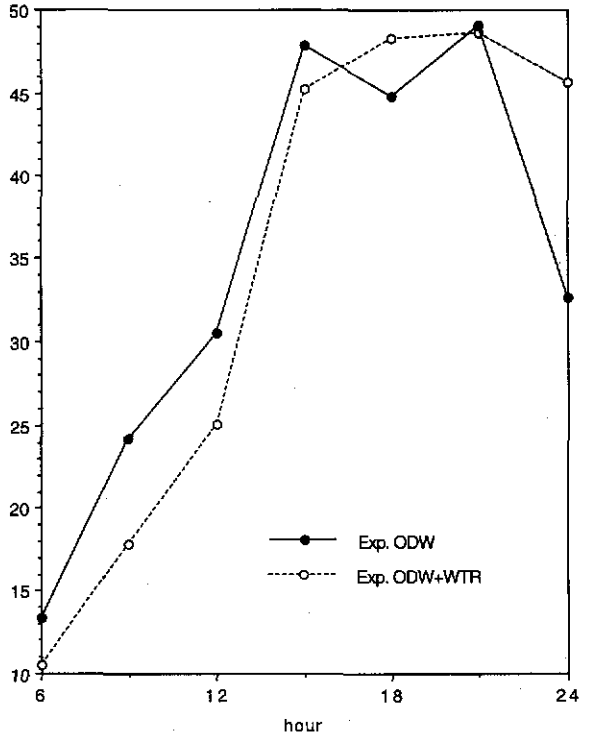

FIG. 22. Horizontal convergence of storm-relative eddy angular momentum between 300 and 700 km radii in the outflow layer for Expts. ODW and ODW+WTR. Units are in 10^{22} g cm^2 s^{-2}.

the cooling of 2 K day^{-1} by eddies remains unchanged between 12 and 18 h in Expt. ODW+WTR. This result again indicates the influence by the approaching westerly UTT and is consistent with the estimate of Molinari and Vollaro (1990).

7. Conclusions and discussion

In this study, model-simulated results were analyzed to reveal the detailed structure of the outflow layer of Florence, and a numerical experiment was performed to study the interactions between the outflow layer of Florence and the upper-level westerlies. Diagnosis of the 200-mb level structure of Expt. ODW at 12 h showed that the outflow layer was highly asymmetric, especially beyond three degrees radius, with an outflow jet originating at approximately three degrees north of the storm center (Fig. 13). The outflow jet was elongated with a length of roughly 2500 km and a width of 500 km. Further diagnosis of the 12-h wind and RH in the outflow jet at the entrance and exit regions of the outflow showed that there was a thermally direct, circum-jet secondary circulation in the entrance region (Fig. 17) and a reversed thermally indirect one in the exit region (Fig. 18). The secondary circulation had an outward branch above the jet, an inward branch below the jet (near 400 mb), an ascending branch in the anticyclonic shear side, and a descending branch in the cyclonic shear side of the outflow jet. The inward branch below the outflow jet in the entrance region of the outflow jet, however, was less apparent in this study than the one shown in Shi et al. (1990).

Because of the complexity due to the existence of other synoptic systems, including the coastal front along the U.S. east coast, it was difficult to isolate a well-defined secondary circulation. In general, the structure of the outflow layer of the simulated Florence was qualitatively similar to the idealized model study in Shi et al. (1990). In their composite study, Chen and Chou (1994) also found a similar jet streak associated with the evolution of upper-tropospheric cold vortices over the western North Pacific during the warm season. They suggested the existence of the circum-jet thermally direct (indirect) secondary circulation in the entrance (exit) region of the jet streak, based on the cloud distribution. This is also consistent with Molinari and Vollaro (1989), in which they speculated that the frontogenetical forcing in the confluence region between the cold trough and the warm hurricane outflow may have enhanced the outflow ahead of the trough via thermal wind adjustment. At 24 h, the westerly jet moved northeastward and was located over Virginia and far away from Florence. However, Florence's center also moved northward and into a region below the south end of the westerly trough. This resulted in the increase of vertical wind shear, the reduction of outflow, and consequently the weakening of the intensity of Florence. At this moment, Florence was about to make landfall. This result is similar to the case described by Holland and Merrill

(1984) where Hurricane Kerry began to decay after the cutoff of the poleward outflow channel.

Calculation of the storm-relative angular momentum budget at 12 h (Table 2) demonstrated that the angular momentum balance was primarily maintained by the Coriolis torque and horizontal transports. It also revealed that the contribution by the horizontal import of eddy cyclonic angular momentum was the dominant feature at large radii, in agreement with the observational study by Molinari and Vollaro (1989). This result again underscored the dominance of the outflow jet in the outflow layer, and the highly asymmetric nature of the outflow layer of tropical cyclones (Black and Anthes 1971).

The most interesting numerical experiment to elucidate the interactions between Hurricane Florence (1988) and its environment is the one in which the approaching westerly UTT was very much weakened (Expt. ODW+WTR). In this numerical experiment, the weakened westerly UTT resulted in a reduction of the maximum speed of the outflow jet of Florence by 6.4 m s^{-1} (or about 15%) at 12 h. The weakened trough and outflow jet of Florence were responsible for a 2-mb minimum SLP increase and a 5.0 m s^{-1} or 13% maximum surface wind reduction. Figure 20 showed that the weakened outflow jet also resulted in weaker convections in the core region in the 10–15 h window, 8–13 h before the model storm reached its maximum intensity. Diagnosis of the 200-mb RH field of this experiment (Fig. 21) indicated a weaker outflow, a weaker and broader thermally direct circulation in the entrance region, and the absence of the thermally indirect circulation in the exit region because of an weaker approaching westerly UTT. The weakened upper-level westerly trough was also responsible for the reduction of inward cyclonic eddy AMF in this numerical experiment (Table 2 and Fig. 22). This result suggested that the large inward flux of cyclonic eddy angular momentum produced by the passage of an upper-level westerly trough was important to the intensification of Florence's inner core convection between 1000 and 1500 UTC 9 September (Fig. 20) and therefore the deepening of the minimum SLP between 1200 and 2400 UTC 9 September. This result also coincided with the cooling of up to 4 K day^{-1} by the eddy heat flux, likely induced by the passage of the upper-level westerly trough at large radii in upper troposphere, at 15 h in Expt. ODW, while the cooling was only 2 K day^{-1} in Expt. ODW+WTR, suggesting the interaction between the upper-level westerly trough and Florence. This result is consistent with the estimate shown in Molinari and Vollaro (1990).

On the other hand, the strong vertical shear associated with the upper-level westerly trough might prevent Florence from further intensifying. Merrill (1988a,b) suggested that the upper-level environmental interactions with tropical cyclones, in general, contribute negatively to intensity changes. His conclusion was based upon two observations: 1) maximum intensity of tropical cyclones is limited by the potential that the sea surface temperature can provide (Emanuel 1986), and tropical cyclones rarely reach to their potential maximum intensity; and 2) increasing vertical shear is usually accompanied by the approach of the upper-level westerly trough and works against the intensification of tropical cyclones. In Florence, however, because it made landfall three hours after it reached maximum intensity, it was difficult to fully determine whether or not the vertical shear associating with the approaching upper-level westerly trough had any negative effect on the intensification. Nevertheless, the result from this numerical experiment suggested that the upper-level westerly trough's contribution was important to the intensification of Florence and the timing and relative position of an approaching westerly UTT and a tropical cyclone is critical for the intensification and decay of a tropical cyclone.

Even though the model-simulated outflow structure of Hurricane Florence is very consistent dynamically and thermodynamically, it remains to be directly verified with observations. Detailed observations of the three-dimensional structure of the outflow layer of tropical cyclones are extremely scarce. The ODW observations used in this study do not provide information above 400 mb, limited by the operational altitude of NOAA WP-3D aircrafts that deployed them. Dropsonde data collected from 200 mb to surface in TCM-90 and TCM-92 experiments (Elsberry and Abbey 1991; Dunnavan et al. 1993) may be very useful in the study of the interactions between the upper-level environment and tropical cyclones. Because Florence made landfall at 0200 UTC 10 September, three hours after it reached its maximum intensity, the window of opportunity for studying interactions between Florence and the upper-level westerly trough is very short (less than a day). Therefore, it is rather difficult to study the full extent of the interactions. A real case study of the interactions between a tropical cyclone and the upper-level environment over an open ocean would be valuable for this purpose, where the timing and relative position of an UTT and a tropical cyclone can be more conveniently analyzed.

Acknowledgments. The authors wish to thank Dr. Keith Sashegyi of the National Research Laboratory (NRL) for his help with the NRL data analysis system and Dr. James Franklin of AOML/HRD for providing the ODW data. We acknowledge many helpful discussions with Dr. Mark DeMaria of AOML/HRD and Dr. Edward Rodgers of NASA/GSFC. This research was supported by an NRL basic research program PE601153N.

REFERENCES

Anthes, R. A., 1974: The dynamics and energetics of mature tropical cyclones. *Rev. Geophys. Space Phys.*, **12**(3), 495–522.

——, 1977: A cumulus parameterization scheme utilizing a one-dimensional cloud model. *Mon. Wea. Rev.*, **105,** 270–286.

Black, P. G., and R. A. Anthes, 1971: On the asymmetric structure of the tropical cyclone outflow layer. *J. Atmos. Sci.*, **28,** 1348–1366.

Challa, M., and R. L. Pfeffer, 1990: The formation of Atlantic hurricanes from cloud clusters and depressions. *J. Atmos. Sci.*, **47,** 909–927.

Chang, S. W., K. Brehme, R. V. Madala, and K. D. Sashegyi, 1989: A numerical study of the East Coast snowstorm of 10–12 February 1983. *Mon. Wea. Rev.*, **117,** 1768– 1778.

Chen, G. T.-J., and L.-F. Chou, 1994: An investigation of cold vortices in the upper troposphere over the western North Pacific during the warm season. *Mon. Wea. Rev.*, **122,** 1436–1448.

Chen, L., and W. M. Gray, 1984: Global view of the upper level outflow patterns associated with tropical cyclone intensity changes during FGGE. Preprints, *15th Conf. on Hurricanes and Tropical Meteorology,* Miami, FL, Amer. Meteor. Soc., 224–231.

DeMaria, M., J.-J. Baik, and J. Kaplan, 1993: Upper-level eddy angular momentum fluxes and tropical cyclone intensity change. *J. Atmos. Sci.*, **50,** 1133–1147.

Detering, H. W., and D. Etling, 1985: Application of the E-ε turbulence model to the atmospheric boundary layer. *Bound.-Layer. Meteor.*, **33,** 113–133.

DiMego, G., 1988: The National Meteorological Center regional analysis system. *Mon. Wea. Rev.*, **116,** 977–1000.

Dunnavan, G. M., R. L. Elsberry, P. A. Harr, E. J. McKinley, and M. A. Boothe, 1993: Overview of the tropical cyclone motion-92 (TCM-92) mini-field experiment. Preprints, *20th Conf. Hurricanes and Tropical Meteorology,* San Antonio, TX, Amer. Meteor. Soc., 1–6.

Elsberry, R. L., and R. F. Abbey Jr., 1991: Overview of the tropical cyclone motion (TCM-90) field experiment. Preprints, *19th Conf. Hurricanes and Tropical Meteorology,* Miami, FL, Amer. Meteor. Soc., 1–6.

Emanuel, K. A., 1986: An air–sea interaction theory for tropical cyclones. Part I: Steady-state maintenance. *J. Atmos. Sci.*, **43,** 585–604.

Frank, W. M., 1977a: The structure and energetics of the tropical cyclone. Part I: Storm structure. *Mon. Wea. Rev.*, **105,** 1119–1135.

——, 1977b: The structure and energetics of the tropical cyclone. Part II: Dynamics and energetics. *Mon. Wea. Rev.*, **105,** 1136–1150.

Franklin, J. L., and M. DeMaria, 1992: The impact of Omega dropwindsonde observations on barotropic hurricane track forecasts. *Mon. Wea. Rev.*, **120,** 381–391.

——, ——, and C. S. Velden, 1991: The impact of Omega dropwindsonde and satellite data on hurricane track forecasts. Preprints, *19th Conf. on Hurricanes and Tropical Meteorology,* Miami, FL, Amer. Meteor. Soc., 87–92.

Holland, G. J., 1983: Angular momentum transports in tropical cyclones. *Quart. J., Roy Meteor. Soc.*, **109,** 187–209.

——, and R. T. Merrill, 1984: On the dynamics of tropical cyclone structural changes. *Quart. J. Roy. Meteor. Soc.*, **110,** 723–745.

Holt, T., S. W. Chang, and S. Raman, 1990: A numerical study of the coastal cyclogenesis in GALE IOP 2: Sensitivity to PBL parameterizations. *Mon. Wea. Rev.*, **118,** 234–257.

Kaplan, J., and J. L. Franklin, 1991: The relationship between the motion of Tropical Storm Florence (1988) and its environmental flow. Preprints, *19th Conf. on Hurricanes and Tropical Meteorology,* Miami, FL, Amer. Meteor. Soc., 93–97.

Kuo, H. L., 1965: On formation and intensification of tropical cyclones through latent heat release by cumulus convection. *J. Atmos. Sci.*, **22,** 40–63.

Lawrence, M. B., and J. M. Gross, 1989: Atlantic hurricane season of 1988. *Mon. Wea. Rev.*, **117,** 2248–2259.

McBride, J., 1981: Observational analysis of tropical cyclone formation. Part III: Budget analysis. *J. Atmos. Sci.*, **38,** 1152–1166.

Madala, R. V., 1981: Efficient time integration schemes for atmospheric and ocean models. *Finite Difference Techniques for Vectorized Fluid Dynamic Calculations,* Springer-Verlag, 56–74.

——, S. W. Chang, U. C. Mohanty, S. C. Madan, R. K. Paliwal, V. B. Sarin, T. Holt, and S. Raman, 1987: Description of the Naval Research Laboratory limited-area dynamical weather prediction model. NRL Tech. Rep. 5992, 131 pp. [NTIS A182780.]

Merrill, R. T., 1984: Structure of the tropical cyclone outflow layer. *Proc. 15th Conf. on Hurricanes and Tropical Meteorology,* Miami, FL, Amer. Meteor. Soc., 421–426.

——, 1988a: Characteristics of the upper-tropospheric environmental flow around hurricanes. *J. Atmos. Sci.*, **45,** 1665–1677.

——, 1988b: Environmental influences on hurricane intensification. *J. Atmos. Sci.*, **45,** 1678–1687.

Molinari, J., and D. Vollaro, 1989: External influences on hurricane intensity. Part I: Outflow layer eddy angular momentum fluxes. *J. Atmos. Sci.*, **46,** 1093–1105.

——, and ——, 1990: External influences on hurricane intensity. Part II: Vertical structure and response of the hurricane vortex. *J. Atmos. Sci.*, **47,** 1902–1918.

Ooyama, K. V., 1987: Numerical experiments of study and transient jets with a simple model of the hurricane outflow layer. Preprints, *17th Conf. on Hurricanes and Tropical Meteorology,* Miami, FL, Amer. Meteor. Soc., 318–320.

Palmen, E., and H. Riehl, 1957: Budget of angular momentum and kinetic energy in tropical cyclones. *J. Meteor.*, **14,** 150–159.

Pfeffer, R. L., 1958: Concerning the mechanisms of hurricanes. *J. Meteor.*, **15,** 113–119.

——, and M. Challa, 1981: A numerical study of the role of eddy fluxes of momentum in the development of Atlantic hurricanes. *J. Atmos. Sci.*, **38,** 2393–2398

Rodgers, E. B., J. Stout, and J. Steranka, 1986: Upper-tropospheric and lower-stratospheric dynamics associated with tropical cyclones as inferred from total ozone measurements. Preprints, *Second Conf. on Satellite Meteorology/Remote Sensing and Applications,* Williamsburg, VA, Amer. Meteor. Soc., 382–387.

——, S. W. Chang, J. Stout, J. Steranka, and J. J. Shi, 1991: Satellite observations of variations in tropical cyclone convection caused by upper-tropospheric troughs. *J. Appl. Meteor.*, **30,** 1163–1184.

Sadler, J. C., 1976: The role of the tropical upper-tropospheric trough in early season typhoon development. *Mon. Wea. Rev.*, **104,** 1266–1278.

——, 1978: Mid-season typhoon development and intensity changes and the tropical upper-tropospheric trough. *Mon. Wea. Rev.*, **106,** 1137–1152.

Sashegyi, K. D., and R. V. Madala, 1993: Application of vertical-mode initialization to a limited-area model in flux form. *Mon. Wea. Rev.*, **121,** 207–220.

Shi, J. J., S. W. Chang, and S. Raman, 1990: A numerical study of the outflow layer of tropical cyclones. *Mon. Wea. Rev.*, **118,** 2042–2055.

——, ——, K. D. Sashegyi, and S. Raman, 1991: Enhancement of objective analysis of Hurricane Florence (1988) with dropsonde data. Preprints, *19th Conf. on Hurricanes and Tropical Meteorology,* Miami, FL, Amer. Meteor. Soc., 335–337.

——, ——, and S. Raman, 1996: Impact of assimilations of dropwindsonde data and SSM/I rain rates on numerical predictions of Hurricane Florence (1988). *Mon. Wea. Rev.*, **124,** 1435–1448.

Steranka, J., E. B. Rodgers, and R. C. Gentry, 1986: The relationship between satellite measured convection burst and tropical cyclone intensification. *Mon. Wea. Rev.*, **114,** 1539–1546.

Tuleya, R. E., and Y. Kurihara, 1981: A numerical study on the effects of environmental flow on tropical storm genesis. *Mon. Wea. Rev.*, **109,** 2487–2506.